

where $b^2 = x^2 + (y/\eta)^2 + (z/\zeta)^2$. They base this profile on fits to the *COBE* *L*-band data, finding $b_m = 1.9$ kpc, $b_0 = 0.1$ kpc, $\eta = 0.5$, and $\zeta = 0.6$.

In order to compute g_N for the bulge, I neglect the triaxiality and use the sphere that is geometrically equivalent to equation (13). This gives the same run of mass with radius, substituting $r/[(\eta\zeta)^{1/3}b_m]$ for b/b_m and similarly for b/b_0 . Then

$$g_{N,\text{bulge}} = \frac{V_{\text{bulge}}^2(R)}{R} = \frac{4\pi G}{R^2} \int_0^R \rho_{\text{bulge}}(r)r^2 dr, \quad (14)$$

which I integrate numerically. The factor $\rho_{\text{bulge},0}$ is scaled to give the correct bulge mass for each choice of scale length (Table 1).

The effects of deviations from this particular bulge model are explored in § 4.1. These details are fairly unimportant here, as they only affect the inner 3 kpc where the motions are noncircular owing to the triaxial distribution of the inner bulge-bar component implied by equation (13). All that matters to the results at $R > 3$ kpc is the total mass enclosed therein.

3.3. The Gas Disk

For the gas, I adopt the distribution given by Olling & Merrifield (2001, their Table D1). I include both the molecular and atomic gas components, treating them as being in a negligibly thin disk. I do not include the ionized gas component for consistency with the treatment of other galaxies. Moreover, this is a very small fraction of the total with an estimated surface density ($1.4 M_\odot \text{ pc}^{-2}$) that is only available at the solar radius.

Olling & Merrifield (2001) give the surface densities scaled by R_0 . For consistency with the Tuorla-Heidelberg model I fix these numbers to $R_0 = 8$ kpc. The surface densities of H_2 and H I gas are corrected upward by a factor of 1.4 to account for the associated mass in helium and metals. For these assumptions, the gas distribution integrates to a total mass $M_{\text{gas}} = 1.18 \times 10^{10} M_\odot$. This is slightly more gas mass than inferred by Flynn et al. (2006) from different data, whose total sums to just under $10^{10} M_\odot$. This seems like an adequate level of agreement considering the diversity of published opinions.

The gas is usually neglected in mass models of the Milky Way as it is a trace component compared to the stars and dark matter halo. However, the gas is not negligible in MOND. The models considered here have gas mass fractions in the range $f_g = M_{\text{gas}}/M_b = 0.19 \pm 0.01$ (Table 1). This is an important component of the total gravitating mass in the absence of dark matter. Effects of the detailed distribution of the gas are reflected in the total rotation curve.

4. THE MILKY WAY ROTATION CURVE

Given the Milky Way mass distribution, MOND predicts the rotation curve. Unlike the case with external galaxies, the mass-to-light ratio is not a fit parameter. The Tuorla-Heidelberg model plus the gas distribution of Olling & Merrifield (2001) specify the mass. The only choices to be made are the scale length and the interpolation function.

Figures 2, 3, and 4 show the results for increasing choices of scale length. In each case, four interpolation functions are illustrated: \hat{v}_1 and \hat{v}_2 (these are practically indistinguishable from the simple and standard interpolation functions), and for comparison the functions \tilde{v}_1 and \bar{v}_1 newly suggested by Milgrom & Sanders (2008). MOND produces a realistic rotation curve given a mass distribution, especially for the shorter scale lengths preferred by the *COBE* data.

As we increase the scale length to $R_d > 3$ kpc, MOND produces less plausible looking rotation curves. In these cases, the bulge causes a prominent peak in the inner rotation curve. Such a morphology is sometimes seen in early-type spirals (Noordermeer et al.

2007), but the sharp peak in Figure 4 is rather unusual. This aspect is sensitive to the bulge model, and more plausible results are possible (§ 4.1).

Comparison with the observed terminal velocities (Kerr et al. 1986; Malhotra 1995) also favors short scale lengths. The agreement is particularly good for \hat{v}_1 when $R_d = 2.3$ kpc. The other interpolation functions are hard to distinguish from one another and seem to prefer slightly longer scale lengths $R_d \approx 2.5$ kpc. This result is sensitive to small changes (of order 4%) in the terminal velocity data (§ 5), so stronger statements seem unwarranted.

The Galactic constants can be computed for each model. Table 2 gives the rotation velocity at the solar circle Θ_0 and the Oort constants A and B :

$$A = \frac{1}{2} \left(\frac{\Theta_0}{R_0} - \frac{dV_c}{dR} \Big|_{R_0} \right), \quad (15a)$$

$$B = -\frac{1}{2} \left(\frac{\Theta_0}{R_0} + \frac{dV_c}{dR} \Big|_{R_0} \right). \quad (15b)$$

The latter depend on the derivative of the rotation curve, which in these models depends somewhat on the extent over which the derivative is measured. That is, there are bumps and wiggles in the rotation curve as a result of the nonsmooth gas distribution (Olling & Merrifield 2001). This causes the derivative to vary in a nontrivial fashion. For specificity, I compute A and B over ± 0.5 kpc around $R_0 = 8$ kpc. One may wonder if this effect has played a role in the various values of the Oort constants that have been derived historically.

The Galactic constants are shown graphically in Figure 5. The measurement of Feast & Whitelock (1997) is most consistent with \hat{v}_1 for $R_d = 2.1$ kpc. Other interpolation functions and scale lengths are possible, depending on how literally we take the error bars. The function \hat{v}_1 seems to perform best, with reasonable values of Θ_0 , A , and B for $R_d \leq 2.5$ kpc. This interpolation function is very similar to the simple function found by Famaey & Binney (2005) to work best in combination with the Basel model.

The other interpolation functions perform less well, although again one must be cautious as always about the interpretation of astronomical uncertainties. For example, \tilde{v}_1 gives reasonable Θ_0 up to $R_d = 3$ kpc, but tends to give $A < |B|$ in contradiction to most measurements. Similarly, \bar{v}_1 gives reasonable B -values, but tends to run low in the other Galactic constants except for the smallest scale lengths. The standard function traditionally used in fitting external galaxies also gives good B -values for all scale lengths, but rather low Θ_0 , albeit within the realm of possibility (Olling & Merrifield 1998).

For all interpolation functions, agreement with both the Galactic constants and the terminal velocities steadily deteriorates with increasing scale length. It therefore seems clear that MOND prefers a Milky Way with a short scale length, $R_d \lesssim 2.5$ kpc. There also seems to be a preference for something closer to the simple interpolation function, as found by Famaey & Binney (2005). It seems quite remarkable that given the mass distribution specified by the Tuorla-Heidelberg model for the stars and Olling & Merrifield (2001) for the gas, MOND produces a plausible rotation curve that is consistent with independent terminal velocity data and the observed Galactic constants with no fitting whatsoever.

4.1. Effects of the Bulge Scale Length

The model constructed here employs the spherical radial profile that is geometrically equivalent to the observed *L*-band light distribution of the central bulge-bar component. This results in a rotation curve for this component that is very similar to that of Englmaier & Gerhard (1999), as it should be since it is based on the same data.

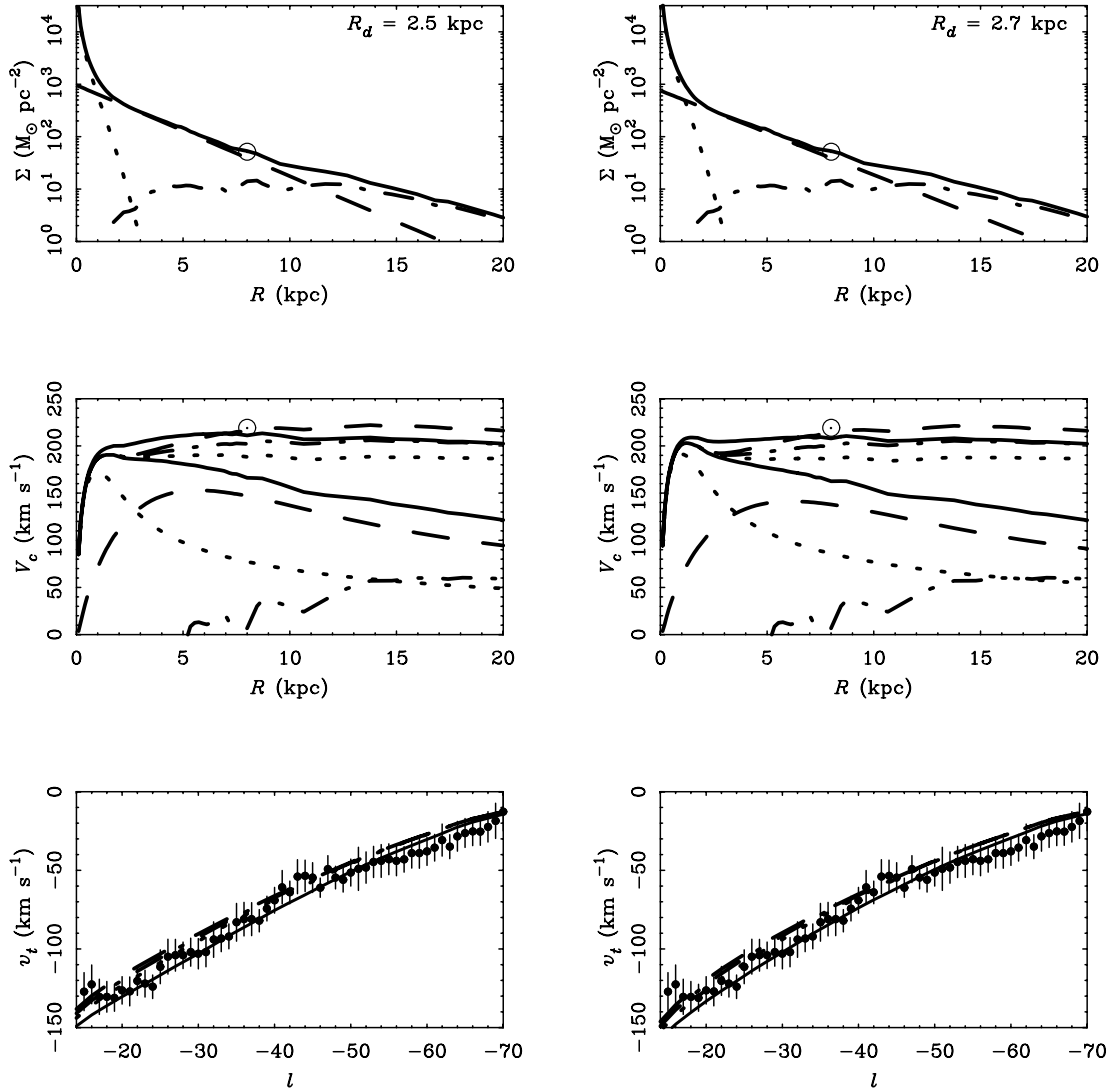


FIG. 3.—Same as Fig. 2, but for $R_d = 2.5$ and 2.7 kpc. [See the electronic edition of the Journal for a color version of this figure.]

$\sim 185 \text{ km s}^{-1}$ at $\sim 50 \text{ kpc}$, asymptoting to $\sim 180 \text{ km s}^{-1}$. Such a gradually declining rotation curve helps to reconcile the apparent (albeit minor) discrepancy between the Milky Way and the Tully-Fisher relation (McGaugh 2005, Flynn et al. 2006; Hammer et al. 2007): Θ_0 is a bit larger than V_f . More importantly, this prediction appears to be consistent with the SDSS data.

Xue et al. (2008) employ Λ CDM simulations to aid in the interpretation of the SDSS data. This is obviously inappropriate for a MONDian analysis. Indeed, one wonders if it is appropriate at all given the difficulties Λ CDM models persistently face on galaxy scales (e.g., Kuzio de Naray et al. 2006; McGaugh et al. 2007). The Milky Way itself is problematic in this regard (Binney & Evans 2001). The baryon distributions of neither the Tuorla-Heidelberg model nor the Basel model tolerate the expected cusp in the dark matter halo. As with other bright spirals, the baryons account for too much of the rotation curve budget at small radii. Hopefully the result of Xue et al. (2008) is dominated by the data and would not change greatly with a different analysis.

5. THE INVERSE PROBLEM: SURFACE DENSITIES FROM VELOCITIES

The Tuorla-Heidelberg model gives very useful constraints on the mass distribution of the Milky Way, but it is still couched in

terms of a smooth exponential disk. Real galaxies deviate somewhat from pure exponentials, and these bumps and wiggles in the surface brightness are reflected in the rotation curve (Renzo's rule: Sancisi 2004; McGaugh 2004). One wonders if this might also be the case for the Milky Way.

Recently, very high quality estimates of the terminal velocities in the fourth quadrant have become available (Luna et al. 2006; McClure-Griffiths & Dickey 2007). These suggest the possibility of reversing the exercise above, and inferring the surface density distribution of the Milky Way from these data. Note that equation (3) can be inverted to obtain the baryonic rotation curve from the observed terminal velocity curve: $V_b = V_c/\sqrt{\nu}$. Then the inversion to surface density becomes a purely Newtonian problem. In principle, this can be accomplished by employing equation (2-174) of Binney & Tremaine (1987):

$$\Sigma(R) = \frac{1}{\pi^2 G} \frac{1}{R} \int_0^R \frac{d^2}{dR} K \frac{u}{R} du + \int_R^\infty \frac{d^2}{dR} K \frac{R}{u} \frac{du}{u}. \quad (16)$$

Note that this procedure should work even in the context of dark matter. If MOND is not correct as a theory, the interpolation

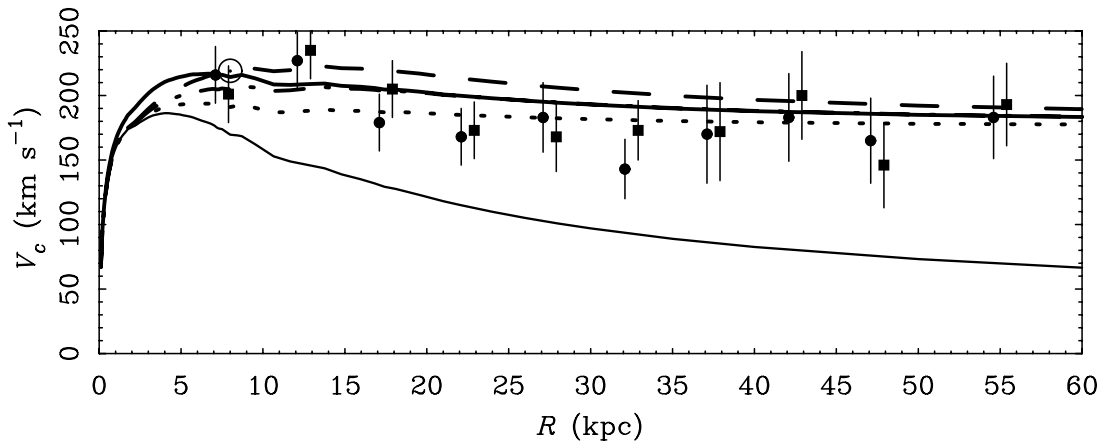


Fig. 7. Outer rotation curve predicted by MOND for the Milky Way compared to the two realizations of the blue horizontal branch stars in the SDSS data report by Xue et al. (2008). The data points from the two realizations have been offset slightly from each other in radius for clarity; the lines are the MOND case illustrated here with $R_0 = 2.3$ kpc, but the rotation curve beyond 15 kpc is not sensitive to this choice. While the data clearly exceed the Newtonian expectation (declining curve), they are consistent with MOND. See the electronic edition of the Journal for a color version of this figure.

tweaking it to bring it closer to the data. The new terminal velocities, which are consistent in shape with the older data, are 8 km s^{-1} higher in amplitude. This appears largely to result from the method by which the maximum line-of-sight velocity is estimated (see extensive discussion in McClure-Griffiths & Dickey 2007). While this hardly seems like a large offset ($\sim 10\%$), it is quite noticeable in MOND. It implies higher surface densities, albeit well within the uncertainties of the Tuorla-Heidelberg model. Given the current interarm location of the Sun, it might even be desirable to have the azimuthally averaged surface density at the solar radius be somewhat higher than the local column.

The case of \tilde{b}_1 with $R_{d1} = 2$ kpc is the smooth case that comes closest to matching the data of Luna et al. (2006) and McClure-Griffiths & Dickey (2007). Starting from this initial guess, I perturb the surface density profile by manually adjusting the surface density in the range necessary to affect the terminal velocity data. To be specific, I match the data of Luna et al. (2006) in the range $3 \text{ kpc} < R < 7.8 \text{ kpc}$. Velocities inside 3 kpc are not perturbed since the motions there are thought to be noncircular, and the details of their choice of bulge model begin to matter (1). For simplicity I assume that the inner distribution is purely exponential, but this does not matter so long as the enclosed mass remains the same. One could just as well imagine a Galaxy with an inner bulge plus a Freeman type II profile that sums to the same mass.

The procedure is to adjust the surface density profile manually, estimating the amount to adjust by the desired ΔV . I then use the routine ROTMOD in GIPSY (van der Hulst et al. 1992) to compute V_b for the perturbed surface density distribution. I compare $V_c = \tilde{a}^{1/2}(y)V_b$ to the data, and repeat the procedure. Although tedious, this procedure can be made to converge with sufficient patience. That is, it is possible to obtain a model that matches the detailed shape of the terminal velocity data.

The result of this procedure is presented in Figure 8. Note that in order to affect the velocity at 3 kpc, it is necessary to start adjusting the surface density somewhere inside of that. The inferred stellar surface densities and corresponding velocities are given in Table 3. Outside of this range, the stellar density remains that of a purely exponential disk. The gas is assumed to follow the distribution of Olling & Merrifield (2001); only the stellar disk has been adjusted. The total mass is 2% higher than the initial pure exponential disk: $M_{\text{disk}} = 5.48 \times 10^{10} M_{\odot}$.

We should be careful not to overinterpret the result. I have only one choice of interpolation function \tilde{a} ; other choices

would give somewhat different results. Moreover, the assumption of circular motion is implicit; streaming motions along the spiral arms are likely to be present at some level. Indeed, Luna et al. (2006) give $V_c(R = 7.8 \text{ kpc}) = 2336 \text{ km s}^{-1}$. This is difficult to reconcile with $V_c(R_0 = 8.0 \text{ kpc}) = 219 \text{ km s}^{-1}$ (Reid et al. 1999) with purely circular motion in any type of model. Variations of this sort are at least conceivable in MOND (Fig. 8), but probably reflect a real difference between the first and fourth quadrants. Hence, I have made no attempt to force a fit to the solar value. The Oort constants of this model are fairly reasonable: $A = 15.9 \text{ km s}^{-1} \text{ kpc}^{-1}$ and $B = 13.0 \text{ km s}^{-1} \text{ kpc}^{-1}$. The value of A may seem a bit high, but note that since the rotation velocity is inferred to be higher than the solar value, B must also be higher. This is in the data. The model fits the detailed terminal velocity curve as far as it is reported (up to $R = 7.8 \text{ kpc}$), so these are in agreement. There is only a modest model-dependent extrapolation to the solar radius. Barring systematic errors in the data or sharp features in the rotation curve near the solar radius, the uncertainty in these estimates is $\sim 1 \text{ km s}^{-1} \text{ kpc}^{-1}$.

Indeed, it is instructive that this exercise can be successfully done at all. The inferred surface density has the sorts of bumps and wiggles commonly observed in the azimuthally averaged surface brightness profiles of spiral galaxies. These correspond to the bumps and wiggles in the rotation curve, as they must in MOND, and as they are observed to do in general (Renzo's rule). This correspondence follows in the dark matter picture only if disks are dynamically important. This is hard to arrange with the cuspy halos obtained in CDM simulations (e.g., Navarro et al. 1997) as these place too much dark mass at small radii. Low surface brightness (LSB) disks cannot have dynamically significant mass in the dark matter picture (de Blok & McGaugh 1997), yet still obey the correspondence of bumps and wiggles encapsulated by Renzo's rule (e.g., Broeils 1992). This occurs naturally in MOND, the a priori predictions of which (Milgrom 1983b) are realized in LSB galaxies (Milgrom & Braun 1988; McGaugh & de Blok 1998). The specific pattern of bumps and wiggles seen in Figure 8 is in principle testable by star count analyses. In particular, it is tempting to associate the dip in surface density at 3 kpc and the subsequent shelf with a ring or spiral arms, perhaps emanating from the end of the long (4.5 kpc) bar (Cabrera-Lavers et al. 2007). A morphology frequently seen in other galaxies and naturally reproduced in MOND simulations (Tiret & Combes 2007).

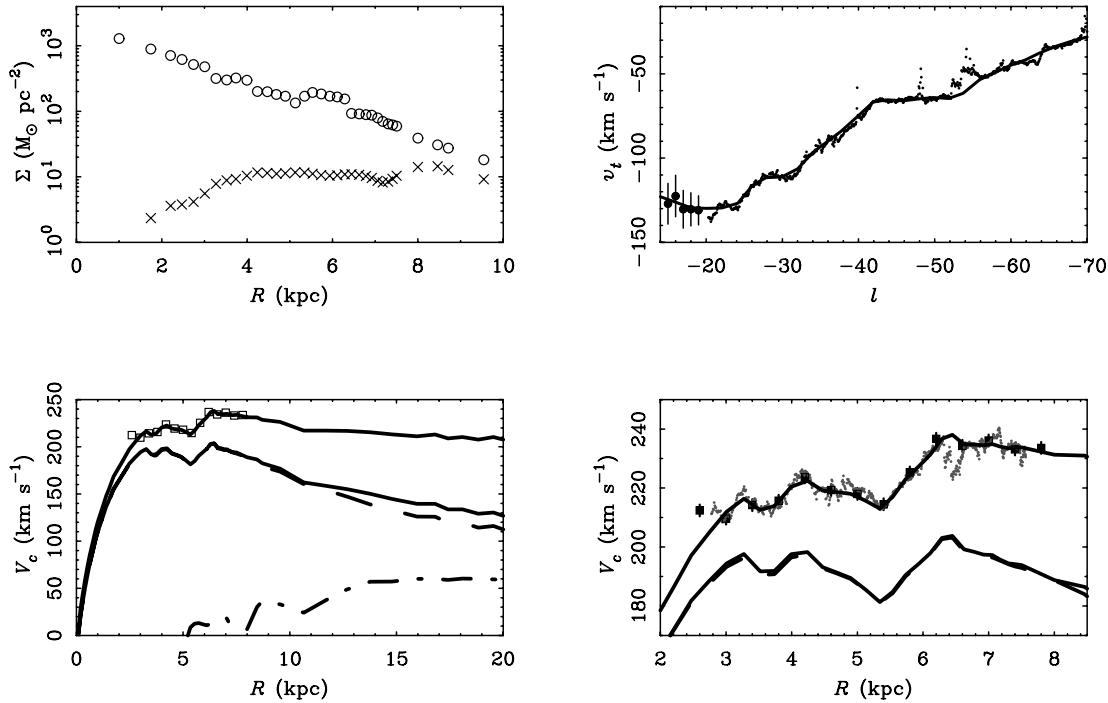


FIG. 8.—Milky Way stellar surface density (*top left, circles*) inferred from the terminal velocity data assuming \hat{v}_1 and the illustrated gas surface densities (*crosses*). The terminal velocities of McClure-Griffiths & Dickey (2007) are shown at top right together with the MOND model fit to the data of Luna et al. (2006). The latter are shown as squares in the bottom panels. The total and component rotation curves are shown as in Fig. 2 at bottom left. At bottom right is a close-up of the fit region with both terminal velocity data sets. The bumps and wiggles in the velocity data can be reproduced, giving features similar to those seen in external galaxies in both $\Sigma(R)$ and $V_c(R)$. [See the electronic edition of the Journal for a color version of this figure.]

TABLE 3
INFERRED SURFACE DENSITIES

R (kpc)	Σ_* ($M_\odot \text{ pc}^{-2}$)	V_c (km s^{-1})
2.47.....	620	197
2.74.....	520	204
3.01.....	480	211
3.27.....	318	216
3.52.....	300	212
3.74.....	323	213
3.99.....	299	220
4.24.....	200	222
4.47.....	199	219
4.69.....	180	218
4.90.....	170	218
5.18.....	135	215
5.34.....	170	213
5.54.....	195	216
5.74.....	185	223
5.94.....	170	227
6.11.....	165	231
6.29.....	155	236
6.45.....	93	238
6.62.....	91	234
6.78.....	89	234
6.92.....	87	234
7.06.....	79	234
7.18.....	70	234
7.30.....	65	233
7.41.....	62	233
7.50.....	59	233

NOTE.—Stellar surface densities outside this range follow an exponential distribution with $R_d = 2.0$ kpc and $\Sigma_0 = 2133 M_\odot \text{ pc}^{-2}$.

Again however, the details of star counts will depend on the choice of interpolation function and the level of noncircular motions. Indeed, even for a given interpolation function and purely circular motion, the result at this level of detail depends on whether we use the modified gravity of Bekenstein & Milgrom (1984; eq. [2]) or modified inertia (eq. [1]). I have implicitly assumed the latter here.

Another intriguing thing to note is that a fit to the surface densities in Table 3 gives $R_d = 2.4$ kpc even though the base model has $R_d = 2.0$ kpc. This type of variation in R_d with the fit radial range is commonly found in external galaxies, and may go some way to explaining the variation in reported scale lengths for the Milky Way (Sackett 1997). Clearly MOND prefers a compact Milky Way, consistent with the *COBE* data (Binney et al. 1997; Drimmel & Spergel 2001) and the rather high observed microlensing optical depth (Popowski et al. 2005) that requires that baryonic mass dominate within the solar circle (Binney & Evans 2001; Bissantz et al. 2004).

A related test of MOND in the Milky Way is provided by the vertical support of the stellar and gas disks. In the outskirts of the Galaxy, the baryonic components should flare substantially as the effective mass scale height comes to be dominated by the quasi-spherical dark matter halo. In contrast, the potential remains disk-like close to the plane in MOND. The net effect is that MONDian disks will be somewhat thinner, all other things being equal.

Recently, Sánchez-Salcedo et al. (2008) have analyzed the thickness of the gas layer of the Milky Way in the context of MOND. They find that MONDian self-gravity of the disk provides a plausible explanation of the thickness and flaring of the gas layer. Milgrom (2008) points out that the form of the interpolation function as well as the mass model matters to the details of the support of the gas layer. It also seems possible that magnetic field support may be nonnegligible, so a perfect fit might be difficult to obtain.

In comparison, it is necessary to invoke a massive ($>10^{11} M_{\odot}$) ring-like dark matter component in addition to the traditional quasi-spherical halo in order to explain the gas thickness in conventional terms (Kalberla et al. 2007).

For stars, MOND will support a higher vertical velocity dispersion at a given disk thickness. This effect in the Milky Way is rather subtle until large radii (Nipoti et al. 2007), but might conceivably be detectable with *Gaia*. The large velocity dispersions of planetary nebulae at large radii in face-on spirals might be an indication of such an effect (Herrmann & Ciardullo 2005).

6. CONCLUSIONS

By treating the Milky Way as we would an external galaxy, it is possible to obtain the rotation curve from the surface density with MOND. There is no freedom to adjust the mass-to-light ratio as in external galaxies. The result is satisfactory provided the scale length of the Milky Way is relatively short (2–2.5 kpc), as implied by the *COBE* data (Binney et al. 1997; Gerhard 2002, 2006). It is also possible to invert the procedure and derive a plausible detailed surface density distribution from the observed terminal velocity curve.

The major conclusions of this work are as follows.

1. Given the observed stellar and gas mass distribution of the Milky Way, MOND naturally produces a plausible rotation curve that is consistent with the relevant dynamical data. This follows with no fitting.

2. MOND prefers Milky Way models with relatively short ($2.0 \text{ kpc} \lesssim R_d \lesssim 2.5 \text{ kpc}$) scale lengths. In this range, rotation curves that look familiar from the study of external galaxies are produced. As the scale length is increased beyond this range, the morphology of the resulting rotation curve becomes less realistic, and the match to kinematic data becomes worse.

3. The Milky Way data seem to prefer an interpolation function close to the simple form, in agreement with the findings of Famaey & Binney (2005). The precise form that is preferred depends on the details of the adopted Milky Way model, so it is unclear how definitive a statement can be made.

4. An interpolation function that shares the virtues of the simple function on galaxy scales without having as large an impact on solar system dynamics is $\hat{v}_1^{-1}(y) = 1 - \exp(-\sqrt{y})$. Other forms are possible. Empirical calibration of this function is desirable, even in the context of dark matter, since it encapsulates the coupling between mass and light.

5. It is possible to recover the detailed surface mass density of the Milky Way from the observed terminal velocities. The result is a Galaxy with bumps and wiggles in both its luminosity profile and rotation curve that are reminiscent of those frequently observed in external galaxies.

6. A prominent feature among the bumps and wiggles is a shelf around $\sim 5.5 \text{ kpc}$. This might correspond to a ring or spiral arms, perhaps extending from the ends of the long bar. Fitting the profile including the bumps and wiggles gives $R_d = 2.4 \text{ kpc}$ even though the mass scale length is 2 kpc.

7. The Oort constants in the fourth quadrant are estimated to be $A = 15.9 \text{ km s}^{-1} \text{ kpc}^{-1}$ and $B = -13.0 \text{ km s}^{-1} \text{ kpc}^{-1}$.

It is hard to imagine that all this could follow from a formula devoid of physical meaning.

The author is grateful for conversations with Moti Milgrom, Garry Angus, and Benoit Famaey, and for constructive input from the referee. The work of S. S. M is supported in part by NSF grant AST 05-05956.

REFERENCES

- Anderson, J. D., Laing, P. A., Lau, E. L., Liu, A. S., Nieto, M. M., & Turyshyn, S. G. 1998, *Phys. Rev. Lett.*, 81, 2858
- Angus, G. W., Famaey, B., & Buote, D. A. 2008, *MNRAS*, 387, 1470
- Angus, G. W., & McGaugh, S. S. 2008, *MNRAS*, 383, 417
- Angus, G. W., Shan, H. Y., Zhao, H. S., & Famaey, B. 2007, *ApJ*, 654, L13
- Begeman, K. G., Broeils, A. H., & Sanders, R. H. 1991, *MNRAS*, 249, 523
- Bekenstein, J. D. 2004, *Phys. Rev. D*, 70, 083509
- . 2006, *Contemp. Phys.*, 47, 387
- Bekenstein, J. D., & Milgrom, M. 1984, *ApJ*, 286, 7
- Binney, J., & Dehnen, W. 1997, *MNRAS*, 287, L5
- Binney, J., & Evans, N. W. 2001, *MNRAS*, 327, L27
- Binney, J., Gerhard, O., & Spergel, D. 1997, *MNRAS*, 288, 365
- Binney, J., & Tremaine, S. 1987, *Galactic Dynamics* (Princeton: Princeton Univ. Press)
- Bissantz, N., Debatista, V. P., & Gerhard, O. 2004, *ApJ*, 601, L155
- Bissantz, N., Englmaier, P., & Gerhard, O. 2003, *MNRAS*, 340, 949
- Bissantz, N., & Gerhard, O. 2002, *MNRAS*, 330, 591
- Bottema, R., Pestaña, J. L. G., Rothberg, B., & Sanders, R. H. 2002, *A&A*, 393, 453
- Bournaud, F., et al. 2007, *Science*, 316, 1166
- Brada, R., & Milgrom, M. 1995, *MNRAS*, 276, 453
- Broadhurst, T., & Barkana, R. 2008, *MNRAS*, submitted (arXiv:0801.1875)
- Broeils, A. H. 1992, *A&A*, 256, 19
- Cabrera-Lavers, A., Hammersley, P. L., González-Fernández, C., López-Corredoira, M., Garzón, F., & Mahoney, T. J. 2007, *A&A*, 465, 825
- Clowe, D., Bradač, M., Gonzalaz, A. H., Markevitch, M., Randall, S. W., Jones, C., & Zaritsky, D. 2006, *ApJ*, 648, L109
- de Blok, W. J. G., & McGaugh, S. S. 1997, *MNRAS*, 290, 533
- . 1998, *ApJ*, 508, 132
- Drimmel, R., & Spergel, D. N. 2001, *ApJ*, 556, 181
- Englmaier, P., & Gerhard, O. 1999, *MNRAS*, 304, 512
- Famaey, B., & Binney, J. 2005, *MNRAS*, 363, 603
- Famaey, B., Bruneton, J.-P., & Zhao, H. 2007, *MNRAS*, 377, L79
- Feast, M., & Whitelock, P. 1997, *MNRAS*, 291, 683
- Felten, J. E. 1984, *ApJ*, 286, 3
- Flynn, C., Holmberg, J., Portinari, L., Fuchs, B., & Jahreiß, H. 2006, *MNRAS*, 372, 1149
- Frinchaboy, P. M. I. 2006, Ph.D. thesis, Univ. Virginia
- Gentile, G., Famaey, B., Combes, F., Kroupa, P., Zhao, H. S., & Tiret, O. 2007, *A&A*, 472, L25
- Gerhard, O. 2002, *Space Sci. Rev.*, 100, 129
- . 2006, *EAS Publ. Ser.*, 20, 89
- Hammer, F., Puech, M., Chemin, L., Flores, H., & Lehnert, M. D. 2007, *ApJ*, 662, 322
- Hayashi, E., & White, S. D. M. 2006, *MNRAS*, 370, L38
- Herrmann, K. A., & Ciardullo, R. 2005, in *AIP Conf. Proc.* 804, *Planetary Nebulae as Astronomical Tools*, ed. R. Szczerba, G. Stasinska, & S. K. Górný (Melville: AIP), 341
- Iorio, L. 2008, *J. Gravitational Phys.*, 2, 26
- Jee, M. J., et al. 2007, *ApJ*, 661, 728
- Kalberla, P. M. W., Dedes, L., Kerp, J., & Haud, U. 2007, *A&A*, 469, 511
- Kerr, F. J., Bowers, P. F., Jackson, P. D., & Kerr, M. 1986, *A&AS*, 66, 373
- Kuzio de Naray, R., McGaugh, S. S., de Blok, W. J. G., & Bosma, A. 2006, *ApJS*, 165, 461
- Luna, A., Bronfman, L., Carrasco, L., & May, J. 2006, *ApJ*, 641, 938
- Malhotra, S. 1995, *ApJ*, 448, 138
- McCarthy, I. G., Bower, R. G., & Balogh, M. L. 2007, *MNRAS*, 377, 1457
- McClure-Griffiths, N. M., & Dickey, J. M. 2007, *ApJ*, 671, 427
- McCulloch, M. E. 2007, *MNRAS*, 376, 338
- McGaugh, S. S. 2004, *ApJ*, 609, 652
- . 2005, *ApJ*, 632, 859
- . 2006, preprint (astro-ph/0606351)
- McGaugh, S. S., & de Blok, W. J. G. 1998, *ApJ*, 499, 66
- McGaugh, S. S., de Blok, W. J. G., Schombert, J. S., Kuzio de Naray, R., & Kim, J. H. 2007, *ApJ*, 659, 149
- Milgrom, M. 1983a, *ApJ*, 270, 365
- . 1983b, *ApJ*, 270, 371
- . 1983c, *ApJ*, 270, 384
- . 1994, *Ann. Phys.*, 229, 384
- . 1999, *Phys. Lett. A*, 253, 273

